http://dx.doi.org/10.5012/bkcs.2014.35.3.961

Size Characterization of Ultrasmall Silver Nanoparticles Using MALDI-TOF Mass Spectrometry†

Byung Hyo Kim, Hogeun Chang, Michael J. Hackett, Jinkyung Park, Pilsun Seo, and Taeghwan Hyeon*

Center for Nanoparticle Research, Institute for Basic Science (IBS), Seoul 151-742, Korea
School of Chemical and Biological Engineering, Seoul National University, Seoul 151-742, Korea
**E-mail: thyeon@snu.ac.kr*
Received October 11, 2013, Accepted November 8, 2013

Key Words : Silver nanoparticle, Ultrasmall nanoparticle, MALDI-TOF, Mass spectrometry

Ultrasmall nanoparticles have recently been the subject of a plethora of research owing to the unique physical and chemical properties manifest in the particles as their size approaches a molecular dispersion.[1-3] Among the ultrasmall nanoparticles, ultrasmall silver nanoparticles were actively researched because of their unique optical and magnetic properties. Although silver is diamagnetic in the bulk state, ultrasmall silver nanoparticles were found to be ferromagnetic.[4] When the size of silver nanoparticles reduces to only a few nanometers, the electronic energy levels become quantized, and the particles emit luminescence.[5] This luminescence has been used as an *in vitro* optical imaging probe.[6] The magnetic and optical properties of ultrasmall silver nanoparticles are highly size-dependent and are derived from the surface of the particle. As particles become smaller in size, the total surface area increases while the core size decreases such that small enough particles may have no core atoms at all.[7] Considering this, the ability to control the functional properties of these particles requires first being able to control the size of the particle during synthesis, and second being able to accurately measure the size distribution. With regard to the latter, microscopic techniques such as transmission electron microscopy (TEM) are the standard for measuring the size of nanoparticles. However, these measurements do not provide accurate estimates of the polydispersity of the total population considering only a very small fraction of particles are observed and measured. Moreover, poor contrast and a tendency for ablation in the electron beam makes the quantification of the total surface area of ultrasmall nanoparticles very difficult.[8] X-ray diffraction (XRD) has been used as an alternative to determine the size of nanoparticles according to the Scherrer equation, but this methods also has inherent inaccuracies because the peak width is also affected by shape and crystallinity. Dynamic light scattering (DLS) is a more accurate sizing technique for nanoparticles, however the low intensity of scattered light induced by ultrasmall particles makes it difficult to characterize these nanoparticles. Recently, mass spectrometry (MS) has been garnering attention in the quantification of particle size.[9-12]

MS has long been one of the most important characterization tools in the fields of chemistry and biology. The spectra are obtained following the ionization of the sample and subsequent sorting based on the mass to charge ratio in magnetic and electric fields. If nanoparticles can be stable under the ionization conditions, the calculated mass provided by MS could then be used to estimate the size of nanoparticles. There are several methods of ionization, the first of which involves subjecting the sample to a large potential causing it to disaggregate (electrospray ionization, ESI). The desorption and ionization process can be assisted by ablation with a high energy laser (matrix assisted laser desorption/ionization, MALDI) or a salvo of inert gases (fast atom bombardment, FAB). For the purpose of quantifying nanoparticles, the particle must remain intact during ionization. Thus, to reduce sample fragmentation, the more mild conditions of MALDI have been extensively used. Particles ionized by MALDI were analyzed by a time of flight (TOF) analyzer which correlates the time it takes from ionization to detection with the mass of the ion. Therefore, MALDI-TOF MS could be employed to characterize ultrasmall nanoparticles as it can quantitate many particles at a time leading to a much better estimate of dispersity. The size range of particles that can be quantified by TOF is very large and highly sensitive. Whetten *et al.* first reported the mass of thiol-capped gold nanoparticles could be measured by MS.[9] ZnS nanoparticles stabilized by *n*-hexadecylamine were analyzed by MS and the results compared to TEM and UV spectroscopy.[10] Recently, Kim et al. obtained the MALDI-TOF mass spectra of 70 batches of ultrasmall iron oxide nanoparticles and provided a size-to-mass conversion equation. This equation is very accurate because it was derived by considering both the mass of the core and that of the ligand.[12] In spite of the recent progress on the measurement of nanoparticles by MS, only a few types of nanoparticles (Au, ZnS, iron oxide) have been investigated by MALDI-TOF MS. This paper will focus on the mass characterization of ultrasmall silver nanoparticles by MALDI-TOF MS and the subsequent conversion of the mass data to size distributions.

Ultrasmall silver nanoparticles were prepared by the previously reported method,[13] and the sizes of several particle

†This paper is to commemorate Professor Myung Soo Kim's honourable retirement.

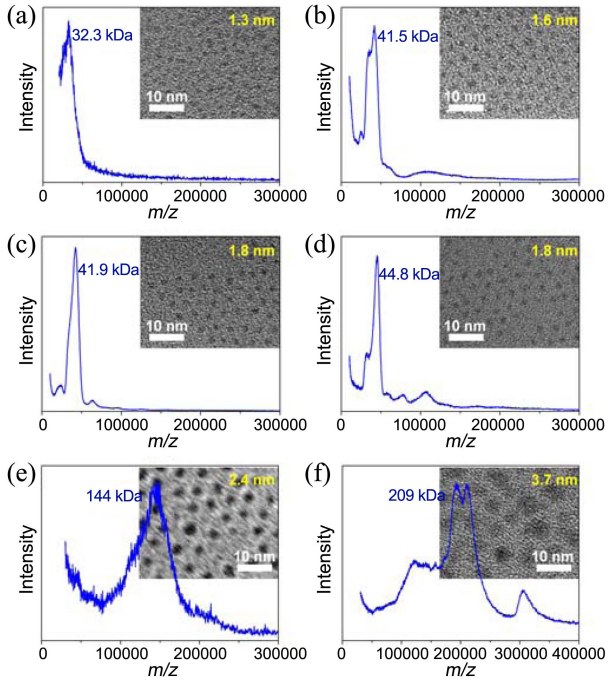

Figure 1. MALDI-TOF mass spectra and corresponding TEM images for various sized ultrasmall silver nanoparticles.

populations were measured from TEM images. The TEM images are presented in Figure 1 and the corresponding particle sizes were measured as 1.3, 1.6, 1.8, 1.8, 2.4, and 3.7 nm, respectively. Because the ultrasmall nanoparticles are hydrophobic, 9-nitroanthracene was selected for the ionization matrix as it allows the hydrophobic nanoparticle to be highly dispersed. In addition, the matrix absorbs the wavelength of the laser source (N_2 laser; 337 nm) and it has a weak interaction with the surface of silver particles. Using 9-nitroanthracene as a matrix, MALDI-TOF mass spectra of ultrasmall nanoparticles were obtained for 1.8 nm silver nanoparticles which correlated to a 41.9 kDa peak (Figure 1(c)).

The correlation function, which converts the mass of a particle into a diameter, was derived from a simple assumption. Because nanoparticles consist of an inorganic core as well as organic ligands, the total mass of the particle can be described as the sum of these masses (*i.e.* $\boldsymbol{M} = \boldsymbol{M}_{\text{core}} + \boldsymbol{M}_{\text{ligand}}$). Assuming the nanoparticle is spherical in shape, the mass of the particle can be expressed as the third order equation with respect to the diameter as described in Eq. (1):

$$\boldsymbol{M} = \rho N_A \cdot \frac{\pi \boldsymbol{D}^3}{6} + \sigma \cdot \pi \boldsymbol{D}^2 = a\boldsymbol{D}^3 + b\boldsymbol{D}^2 \tag{1}$$

In this equation, ρ is the density of the core (1.05×10^{-20} g/nm^3 for silver), N_A is Avogadro's number (6.02×10^{23} mol^{-1} = Da/g), $\boldsymbol{D}$ is diameter of a nanoparticle (nm), σ is surface density of ligands (Da/nm^2). All of the coefficients are known except σ. The surface density can be acquired from the core weight fraction (f) which can be measured by thermogravimetric analysis (TGA). The core fraction is represented by the function of σ as follows in Eq. (2):

$$f = \frac{\boldsymbol{M}_{\text{core}}}{\boldsymbol{M}} = \frac{\rho N_A \cdot \frac{\pi \boldsymbol{D}^3}{6}}{\rho N_A \cdot \frac{\pi \boldsymbol{D}^3}{6} + \sigma \cdot \pi \boldsymbol{D}^2} \tag{2}$$

Eq. (2) can be rearranged to Eq. (3) as follows:

$$\sigma = \frac{\rho N_A D(1-f)}{6f} \tag{3}$$

The σ value was then calculated from the TGA (f) and TEM (D) data. The surface ligand density was 3.13×10^3 Da/nm^2 and it was nearly constant (Table S1). By substituting the σ value into Eq. (1), the third (a) and second (b) order coefficients of $\boldsymbol{D}$ were obtained: $a = 3.31 \times 10^3$ Da/nm^3, $b = 9.82 \times 10^3$ Da/nm^2. The size could then be represented as a function of mass by rearranging Eq. (1) using Cardano's method as follows in Eq. (4):

$$\boldsymbol{D} = \alpha + \sqrt[3]{\alpha^3 + \beta\boldsymbol{M} + \sqrt{2\alpha^3\beta\boldsymbol{M} + \beta^2\boldsymbol{M}^2}} + \sqrt[3]{\alpha^3 + \beta\boldsymbol{M} - \sqrt{2\alpha^3\beta\boldsymbol{M} + \beta^2\boldsymbol{M}^2}} \tag{4}$$

where $\alpha = -2\sigma/\rho N_A \approx -0.990$ (nm) and $\beta = 3/\rho N_A \pi \approx 1.51 \times 10^{-4}$ (nm^3/Da). A plot of Eq. (4) for silver particles is presented in Figure 2. Using Eq. (4), the particle size can be easily estimated from mass data obtained with MALDI-TOF MS. The size of ultrasmall silver nanoparticles having a 41.9 kDa mass is 1.66 nm, and the size of a 44.8 kDa nanoparticle is 1.70 nm which correlates well with the size estimated from TEM (1.8 nm each). The 2.9 kDa difference from the mass data turns out to be 0.04 nm, demonstrating the high sensitivity of MS. This sensitivity is derived from the third order relationship of diameter and mass.

Although the surface ligand density was assumed to be constant, it is known to be affected by the microenvironment at the interface of the surface and the solvent. To investigate the effects of variable surface ligand density on Eq. (4), the

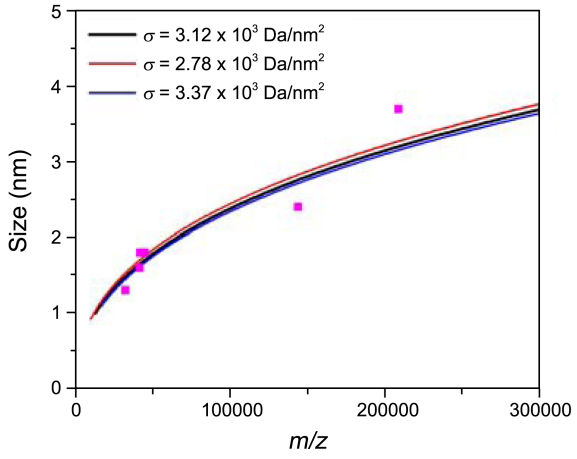

Figure 2. Solid curves indicate the size-to-mass correlation equation in different surface ligand density (black: 3.12; red: 2.78; blue: 3.37 × 10^3 Da/nm^2) from Eq. (4). The position of each pink dot indicates the mass peak position (x-axis) and the mean diameter measured from TEM images in Figure 1.

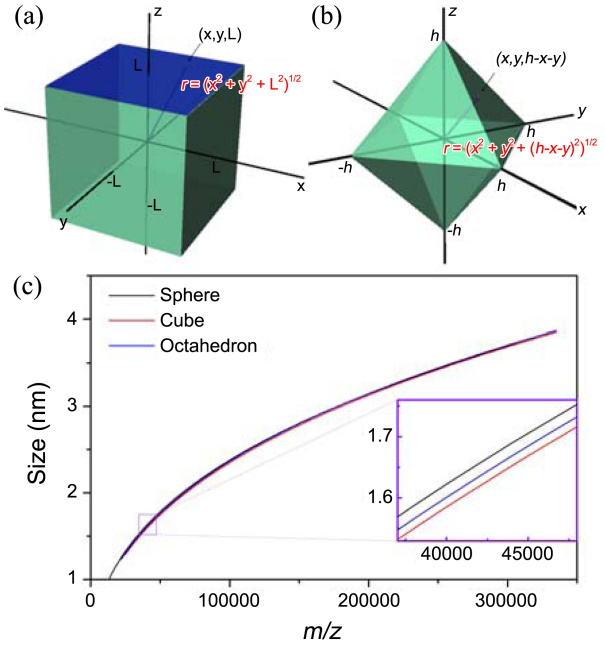

Figure 3. (a) Cube and (b) octahedron models in the rectangular coordinates. (c) Mass-to-size estimation curves for spherical, cubic, and octahedral silver nanoparticles.

maximum and minimum values of surface ligand density (Table S1) were applied to the calculation in the case of ultrasmall silver nanoparticles. The observed surface ligand densities ranged from 2.78×10^3 Da/nm^2 to 3.37×10^3 Da/nm^2, thus the corresponding b coefficients in Eq. (4) would range from 8.73×10^3 Da/nm^2 to 1.06×10^4 Da/nm^2, respectively (Table 1). The correlation curves for these two scenarios are depicted in Figure 2. By employing the range of the surface ligand density, the mass of the particles may be used to calculate a size range. For example, a 41.9 kDa nanoparticle would have an estimated maximum diameter of 1.71 nm ($\sigma = 2.72 \times 10^3$ Da/nm^2) and a minimum diameter of 1.62 nm ($\sigma = 3.22 \times 10^3$ Da/nm^2). This predicted range is smaller than 1 Å, suggesting minor changes in the surface ligand density can be ignored when calculating the particle size by MALDI-TOF MS.

The size-to-mass correlation equation (Eq. 4) can also be applied to non-spherical nanoparticles. However, it is very difficult to synthesize anisotropic ultrasmall nanoparticles so the particles were modeled to compare them with the spherical particles. Since silver particles have a cubic crystal lattice, we modeled cube- or octahedron-shaped nanoparticles (Figure 3(a), (b)). According to Figure 3(a), the total mass (sum of core and ligand masses) of cubic nanoparticles can be described as follows in Eq. (5):

$$\boldsymbol{M} = \rho N_A (2L)^3 + \sigma m \cdot 6 \cdot (2L)^2 \tag{5}$$

In this equation, L is half of the edge length (intercept of cube, see Figure 3(a)). It is necessary to convert the edge length to an average diameter in order to compare the equation with the spherical particles. To do this, the root mean square radius was substituted for the mean radius because the calculation of the average diameter of cube is extremely arduous. The root mean square radius of the top face of cube was also calculated (blue color in Figure 3(a)).

$$\sqrt{\langle \boldsymbol{r} \rangle^2} = \sqrt{\frac{\int_{-L}^{L}\int_{-L}^{L} \boldsymbol{r}^2 dxdy}{\int_{-L}^{L}\int_{-L}^{L} dxdy}} = \sqrt{\frac{\int_{-L}^{L}\int_{-L}^{L} \left(\sqrt{x^2+y^2+\boldsymbol{L}^2}\right)^2 dxdy}{\int_{-L}^{L}\int_{-L}^{L} dxdy}} = \sqrt{\frac{5}{3}}\boldsymbol{L} \tag{6}$$

$$\boldsymbol{D} \approx 2\sqrt{\langle \boldsymbol{r} \rangle^2} = 2\sqrt{\frac{5}{3}}\boldsymbol{L} \tag{7}$$

The result can be regarded as the root mean square radius of the cube considering the six faces of cube are equivalent. Substituting Eq. (7) into Eq. (5), the total mass of the nanoparticles is expressed as a third order formula with respect to the diameter as follows in Eq. (8):

$$\boldsymbol{M} = \left(\frac{3}{5}\right)^{\frac{3}{2}} \rho N_A \boldsymbol{D}^3 + \frac{18}{5}\sigma m \boldsymbol{D}^2 = a\boldsymbol{D}^3 + b\boldsymbol{D}^2 \tag{8}$$

Eq. (8) can be rearranged using Cardano's method resulting in the cubic-equivalent of Eq. (4) with coefficient values of $\alpha = -2\sqrt{5}\,\sigma/\sqrt{3}\,\rho N_A$ and $\beta = 5\sqrt{5}/6\sqrt{3}\,\rho N_A \pi$. For ultrasmall cubic silver nanoparticles, the coefficients α and β are estimated to be −1.28 (nm) and 1.70×10^{-4} (nm^3/Da), respectively (Table 1).

The size-to-mass conversion equation for octahedral nanoparticles was similarly derived for cubic particles. The total mass ($\boldsymbol{M}$) is denoted as follows in Eq. (9):

$$\boldsymbol{M} = \rho N_A \cdot \frac{4}{3}h^3 + \sigma m \cdot 8 \cdot 2\sqrt{3}h^2 \tag{9}$$

In this equation, h is half the axis length (intercept of Figure

Table 1. Coefficient of Eq. (4) in different surface density and shape

Graph	Core density (10^{-20} g/nm^3)	Surface density (10^3 Da/nm^2)	shape	a (10^3 Da/nm^3)	b (10^3 Da/nm^2)	α (nm)	β (10^{-4} nm^3/Da)	Calculated size at 41.9 kDa (nm)	Calculated size at 100 kDa (nm)
Fig. 2, 3	1.05	3.13	Sphere	3.31	9.82	-0.990	1.51	1.66	2.38
Fig. 2	1.05	**2.78**	Sphere	3.31	8.73	-0.879	1.51	1.71	2.44
Fig. 2	1.05	**3.37**	Sphere	3.31	10.6	-1.07	1.51	1.62	2.33
Fig. 3	1.05	3.13	**Cube**	2.94	11.3	-1.28	1.70	1.62	2.34
Fig. 3	1.05	3.13	**Octahedron**	2.98	10.8	-1.21	1.68	1.63	2.37

3(b)). The root mean square radius can be calculated by using one face of the octahedron.

$$\sqrt{\langle \boldsymbol{r} \rangle^2} = \sqrt{\frac{\int_0^{\boldsymbol{h}}\int_0^{\boldsymbol{h}-y} \boldsymbol{r}^2 dxdy}{\int_0^{\boldsymbol{h}}\int_0^{\boldsymbol{h}-y} dxdy}} = \sqrt{\frac{\int_0^{\boldsymbol{h}}\int_0^{\boldsymbol{h}-y} \left(\sqrt{x^2+y^2+(\boldsymbol{h}-x-y)^2}\right)^2 dxdy}{\int_0^{\boldsymbol{h}}\int_0^{\boldsymbol{h}-y} dxdy}} \quad (10)$$

$$\boldsymbol{D} \approx 2\sqrt{\langle \boldsymbol{r} \rangle^2} = \sqrt{2}\boldsymbol{h} \quad (11)$$

The result can be regarded as the total root mean square radius as all eight faces of octahedron are equivalent. Substituting Eq. (11) into Eq. (9), the total mass of the nanoparticles can be expressed as a third order formula with respect to the diameter as follows in Eq. (12):

$$\boldsymbol{M} = \frac{\sqrt{2}}{3}\rho N_A \boldsymbol{D}^3 + 2\sqrt{3}\sigma m \boldsymbol{D}^2 = a\boldsymbol{D}^3 + b\boldsymbol{D}^2 \quad (12)$$

After rearrangement of Eq. (12) into the octahedral-equivalent of Eq. (4), coefficient values of $\alpha = -\sqrt{6}\,\sigma/\rho N_A$ and $\beta = 3/2\sqrt{2}\,\rho N_A \pi$ were obtained. For octahedral silver nanoparticles, the coefficients α and β are estimated to be −1.21 (nm) and 1.68×10^{-4} (nm^3/Da), respectively (Table 1).

The solution of the size-to-mass conversion equations for cubic, octahedral and spherical particles are plotted in Figure 3(c). Although the equations were derived using the root mean square radius, the resulting equations for the cubic and octahedral particles are very similar to the spherical particles. Consequently, it is expected the size-to-mass conversion equation can also be adopted for the analysis of cubic or octahedral nanoparticles.

In conclusion, MALDI-TOF mass spectra of spherical silver nanoparticles in 9-nitroanthracene were successfully used to estimate the corresponding particle sizes. The mass data were converted into a size distribution using a derived equation which correlated well with the sizes measured by TEM. Despite the fact the coefficients of the size-to-mass equation are not constant in ultrasmall nanoparticles, the resulting differences are negligible. Furthermore, this equation should be compatible not only with spherical particles but also with anisotropic particles such as cubic- or octahedral-shaped particles. This suggests MALDI-TOF MS could be used as a generic methodology for estimating the particle size distribution of nanoparticles with various shapes and sizes with high accuracy making it a very valuable and versatile technique in nanotechnology.

Experimental

Synthesis of Silver Nanoparticles. 0.17 g of silver nitrate (Strem Chemical) was added to 0.5 mL of oleylamine (Acros Organics) and 4.5 mL of oleic acid (Sigma-Aldrich Inc.). The mixture was degassed at 70 °C for 90 min under vacuum and the reaction vessel was purged with argon. For the synthesis of 1.8 nm-sized nanoparticles, the solution was heated to 180 °C at a heating rate of 10 °C/min and maintained for 2 min. For 3.7 nm-sized nanoparticles, the heating rate was set to 1 °C/min and the reaction was stopped when the temperature just reached 180 °C. After the reaction, the reaction vessel was cooled to room temperature and washed with 10 mL of toluene and 50 mL ethanol. The nanoparticles were dispersed in chloroform.

Characterization. MALDI-TOF MS was performed on a Voyager-DE™ STR Biospectrometry Workstation (Applied Biosystems). Nanoparticles dispersed in chloroform were mixed with 9-nitroanthracene dissolved in chloroform (Sigma-Aldrich Inc.) in a weight ratio of 1:1 and spotted onto a target plate. The mass spectra were obtained with the 40-50% of the laser's full power. All of the mass spectra were smoothed with a simple average of 100 data points. TEM images were taken with a JEOL-2010 electron microscope and TGA data were collected with a Q-5000 IR (TA Instrument).

Acknowledgments. This work was supported by Institute for Basic Science (IBS).

Supporting Information. TGA data and corresponding TEM images, calculated surface ligand density.

References

1. Gatteschi, D.; Fittipaldi, M.; Sangregorio, C.; Sorace, L. *Angew. Chem., Int. Ed.* **2012**, *51*, 4792.
2. Harrell, S. M.; McBride, J. R.; Rosenthal, S. J. *Chem. Mater.* **2013**, *25*, 1199.
3. Kim, B. H. *et al. J. Am. Chem. Soc.* **2011**, *133*, 12624.
4. Garitaonandia, J. S. *et al. Nano Lett.* **2008**, *8*, 661.
5. Yuan, X.; Luo, Z.; Yu, Y.; Yao, Q.; Xie, J. *Chem. Asian J.* **2013**, *8*, 858-871.
6. Yu, J.; Patel, S. A.; Dickson, R. M. *Angew. Chem., Int. Ed.* **2007**, *46*, 2028.
7. Nützenadel, C.; Züttel, A.; Chartouni, D.; Schmid, G.; Schlapbach, L. *Eur. Phys. J. D* **2000**, *8*, 245.
8. Wilcoxon, J. P.; Martin, J. E.; Provencio, P. *Langmuir* **2000**, *16*, 9912.
9. Whetten, R. L. *et al. Adv. Mater.* **1996**, *8*, 428.
10. Khitrov, G. A.; Strouse, G. F. *J. Am. Chem. Soc.* **2003**, *125*, 10465.
11. Kasuya, A. *et al. Nat. Mater.* **2004**, *3*, 99.
12. Kim, B. H. *et al. J. Am. Chem. Soc.* **2013**, *135*, 2407.
13. Park, J.; Kwon, S. G.; Jun, S. W.; Kim, B. H.; Hyeon, T. *ChemPhysChem* **2012**, *13*, 2540.